Sādhanā Vol. 26, Part 6, December 2001, pp. 517–528. © Printed in India

Modelling flow through unsaturated zones: Sensitivity to unsaturated soil properties

K S HARI PRASAD*, M S MOHAN KUMAR and M SEKHAR

Department of Civil Engineering, Indian Institute of Science, Bangalore 560 012, India
* Present address: Department of Civil Engineering, Indian Institute of Technology, Roorkee 247 667, India
e-mail: msmk@civil.iisc.ernet.in

MS received 13 October 1997; revised 20 November 2001

Abstract. A numerical model to simulate moisture flow through unsaturated zones is developed using the finite element method, and is validated by comparing the model results with those available in the literature. The sensitivities of different processes such as gravity drainage and infiltration to the variations in the unsaturated soil properties are studied by varying the unsaturated parameters α and n over a wide range. The model is also applied to predict moisture contents during a field internal drainage test.

Keywords. Unsaturated zone; capillary fringe; finite element method.

1. Introduction

Moisture flow in the unsaturated zone is an important topic in several branches of hydrology, soil science and agricultural engineering dealing with subsurface flow and transport processes. Water movement through the unsaturated zone is commonly analysed by solving Richard's equation (Richard 1931). Analytical and simplified solutions of Richard's equation (Phillip 1969; Parlange 1972; Broadbridge & White 1988; Warrick *et al* 1991) provide useful tools for studying simple unsaturated flow systems with relatively simple initial and boundary conditions. The solutions of these models are based on the following assumptions: (i) the soil is homogeneous, (ii) the initial moisture content is uniform throughout the soil profile, and (iii) the moisture content at the soil surface is constant and near saturation or rainfall or irrigation rate is constant. In addition, models give accurate results only for a particular type of soil. Fort example, Green-Ampt Model which is based on the assumption of saturated plug flow fails in situations where a coarse textured soil with high hydraulic conductivity underlies a fine textured soil with low hydraulic conductivity (Chow 1988; Chow *et al* 1988). In the field, soils are seldom homogeneous, initial moisture content is seldom uniformly distributed and in most field situations during rainfall or irrigation, the soil surface is rarely at constant saturation. For accurate prediction of moisture movement under realistic boundary conditions in field soils, one has to resort to numerical models which are versatile in handling the nonhomogeneity and different kinds of boundary conditions. Accurate prediction of moisture movement is very

essential in studies concerning transport of hazardous materials such as pesticides, fertilizers and radioactive wastes.

Several numerical models have been developed for simulating water movement in unsaturated porous media using finite difference, finite element, and integrated finite difference methods (Neuman 1973; Narasimhan & Witherspoon 1977; Cooley 1983; Huyakorn *et al* 1986; Hills *et al* 1989; Gottardi & Venutelli 1992). Most of the numerical models considered focus their attention either on improving the existing methods or on concentrating on one process such as infiltration, gravity drainage or evaporation. However, very few attempts have been made to study the sensitivity of different processes with respect to the unsaturated soil parameters. The objective of the present study is to develop a numerical model to simulate water flow through unsaturated zones and study the effect of unsaturated soil parameters on water movement during different processes such as gravity drainage and infiltration.

2. Modelling Richards equation for vertical unsaturated flow

For one-dimensional vertical flow in unsaturated soil, the pressure-head based Richards equation is

$$\frac{\partial}{\partial z}\left[K(\psi)\left(\frac{\partial \psi}{\partial z}+1\right)\right]=C(\psi)\frac{\partial \psi}{\partial t}, \tag{1}$$

where χ is the pressure head, z the vertical co-ordinate taken positive upwards, t time, K the hydraulic conductivity, $C(=\mathrm{d}u/\mathrm{d}c)$ the soil moisture capacity and v the volumetric moisture content. In order to solve (1), constitutive relationships between the dependent variable c and the nonlinear terms K and C have to be specified. In this study, the following constitutive relationships proposed by van Genuchten (1980) are used which are as follows.

θ–ψ Relationship

$$S_e=\left[1/(1+|\alpha\psi|^n)\right]^m, \tag{2}$$

where α and n are unsaturated soil parameters with $m=1-(1/n)$ and S_e is the effective saturation defined as

$$S_e=(\theta-\theta_r)/(\theta_s-\theta_r), \tag{3}$$

where θ_s and θ_r are saturated moisture content and residual moisture content of the soil respectively.

K–θ Relationship

$$K=K_s S_e^{1/2}\left[1-\left(1-S_e^{1/m}\right)^m\right]^2, \tag{4}$$

where K_s is the saturated hydraulic conductivity.

3. Numerical scheme

To solve (1), Galerkin finite element discretisation in space and finite difference discretisation in time is used.

3.1 Spatial discretisation

The solution domain is discretised into $M-1$ elements, each of length Δz, defining M global nodes and the pressure head ψ is approximated as,

$$\psi(z,t) = \hat{\psi}(z,t) = \sum_{m=1}^{M} \psi_{\mathrm{m}}(t) N_{\mathrm{m}}(z), \tag{5}$$

where $\psi m(t)$ are unknown global nodal values of ψ and $N_m(z)$, the corresponding linear Lagrangian basis functions. The method of weighted residuals is used to solve for the unknown nodal values of ψ. The Galerkin formulation applied to (1) yields the system of ordinary differential equations

$$A(\Psi)\Psi + F(\Psi)\frac{\mathrm{d}\Psi}{\mathrm{d}t} + b(\psi) - q(t) = 0, \tag{6}$$

where Ψ is the vector of unknown coefficients corresponding to the values of pressure head at each node, q contains the specified flux boundary conditions at lower and upper boundary and A, F and b are given over local sub-domain element $\Omega^{(e)}$ as

$$\begin{aligned} A^{(e)} &= \int_{\Omega^{(e)}} K^{(e)} \frac{\partial N_1^{(e)}}{\partial z} \frac{\partial N_m^{(e)}}{\partial z} dz, \\ F^{(e)} &= \int_{\Omega^{(e)}} C^{(e)} N_1^{(e)} N_m^{(e)} dz, \\ b^{(e)} &= \int_{\Omega^{(e)}} K^{(e)} \frac{\partial N_1^{(e)}}{\partial z} dz. \end{aligned} \tag{7}$$

In local co-ordinate space, $-1 \le \varepsilon \le 1$, the two element basis functions $N_l^{(e)}$ and $N_m^{(e)}$ are given by

$$\begin{aligned} N_1^{(e)} &= \frac{1}{2}(1-\varepsilon), \\ N_m^{(e)} &= \frac{1}{2}(1+\varepsilon), \end{aligned} \tag{8}$$

with

$$\varepsilon = 2\left(z - z_c^{(e)}\right)/\Delta z^{(e)},$$

where z is the co-ordinate of any point in the sub-domain element $\omega^{(e)}$, $z_c^{(e)}$ and $\Delta z^{(e)}$ being the coordinate of the mid-point and the length of the element $\Omega^{(e)}$ respectively. The nonlinear integrals in (7) are evaluated using second-order Gaussian quadrature. For linear Lagrangian basis functions, A and F have banded structures with a band width of three.

3.2 Time differencing

Introducing a backward finite difference discretisation of the time derivative term, (6) can be written as

$$A\left(\Psi^{k+\lambda_t}\right)\Psi^{k+\lambda_t} + F\left(\Psi^{k+\lambda_t}\right)\left(\Psi^{k+1} - \Psi^{k}\right)/\Delta t + b\left(\Psi^{k+\lambda_t}\right) - q\left(\Psi^{k+\lambda_t}\right) = 0, \tag{9}$$

where

$$\Psi^{k+\lambda_t} = \lambda_t \Psi^{k+1} + \left(1 - \lambda_t\right)\Psi^k, \quad \text{with} \quad 0 \leq \lambda_t \leq 1. \tag{10}$$

In (9), superscript k denotes the time level, Δt denotes the time step and λt denotes the time weighting or relaxation parameter.

Equations (9) are nonlinear in Ψ^{k+1}, except when $\lambda_t = 0$. Some iterative or linearisation strategy is required to solve such equations. Paniconi *et al* (1991) evaluated the performance of various iterative and non-iterative methods for the solution of (9) . In this study the Picard iterative scheme is used .

3.3 Picard scheme

The Picard scheme is implemented on (9), by iterating with all nonlinear terms evaluated at the previous iteration level, p, i.e,

$$\left(\lambda_t A^{k+\lambda_t,p} + 1/\Delta t \; F^{k+\lambda_t,p}\right) \Psi^{k+1,p+1} = q^{k+\lambda_t,p} - b^{k+\lambda_t,p} - (1-\lambda_t) A^{k+\lambda_t,p}\Psi^k + 1/\Delta t\, F^{k+\lambda_t,p}\Psi^k. \tag{11}$$

Equation (11) can be written in the form

$$\left(\lambda_t A^{k+\lambda_t,p} + 1/\Delta t\, F^{k+\lambda_t,p}\right) \Delta\Psi^{k+1,p+1} = -f\left(\Psi^{k+1,p}\right), \tag{12}$$

where

$$\Delta\Psi^{k+1,p+1} = \Psi^{k+1,p+1} - \Psi^{k+1,p}, \tag{13}$$

and

$$f\left(\Psi^{k+1,p}\right) = \lambda_t A^{k+\lambda_t,p}\Psi^{k+1,p} + \left(1-\lambda_t\right)A^{k+\lambda_t,p} + F^{k+\lambda_t,p}\left((\Psi^{k+1,p} - \Psi^k)/\Delta t\right) + b^{k+\lambda_t,p} - q^{k+\lambda_t,p}. \tag{14}$$

Equation (12) is applicable in the same form while considering Neumann type (specified flux) boundary conditions. However modifications to (12) are necessary for considering a Dirichlet type (specified pressure head) condition. In such situations, the coefficient matrix and the right hand side of (12) should be suitably modified. The diagonal term of the row corresponding to the Dirichlet node in the coefficient matrix of (12) is set to unity while the off-diagonal terms of the row corresponding to the Dirichlet node are set to zero. In the right hand vector, the elements corresponding to the Dirichlet node are also set to zero. The system of (12) is tridiagonal in nature and which can be solved conveniently by a direct decomposition method called double sweep method or Thomas algorithm (Remson *et al* 1971). Convergence in the iterative scheme is monitored by computing the maximum error norm $\left|\Delta\Psi^{k+1,p+1}\right|_\infty$. Convergence is achieved when norm falls below some specified tolerance level .

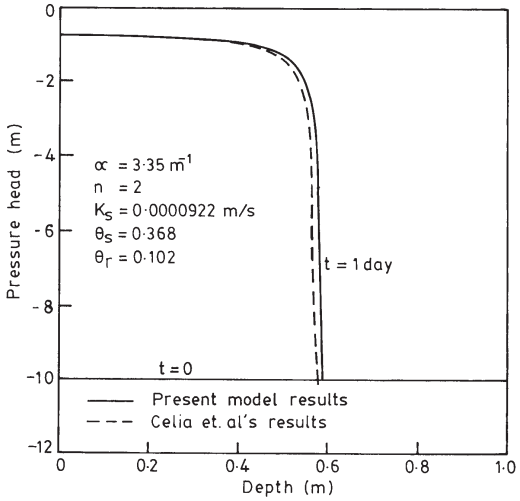

Figure 1. Comparison of results – Celia's problem.

4. Model validation

The finite element model is validated by comparing the model results with a problem chosen from the literature. The problem considers infiltration of a homogeneous soil column which is initially dry (Celia *et al* 1990). The soil parameters are $\alpha = 3.35\,\mathrm{m}^{-1}$, $n = 2$, $K_s = 9.22 \times 10^{-5}$ m/s, $\theta_s = 0.368$ and $\theta_r = 0.102$. The length (L) of the soil sample is 1 m.

The initial and boundary conditions are:

$$\begin{aligned} t = 0; &\qquad \Psi = -10\,\mathrm{m}, &&\qquad 0 \le z \le 1\,\mathrm{m}, \\ t > 0; &\qquad \Psi = -10\,\mathrm{m}, &&\qquad z = 0. \\ t > 0; &\qquad \Psi = -0.75, &&\qquad z = 1\,\mathrm{m}. \end{aligned}$$

Celia *et al* (1990) obtain finite element as well as finite difference solutions using coarse and fine grid approximations . The problem is simulated using the present model with fine grid approximation ($\Delta z = 1$ cm and $\Delta t = 1$ s). The pressure heads after one day simulation are compared with the fine grid solution of Celia *et al* (1990). It can be seen from figure 1 that both the results match well, indicating the validity of the model. The mass balance error is less than 1%. The minor deviation observed in figure 1 between the two model results may be due to the error in presenting the simulated results from Celia *et al* (1990).

5. Sensitivity analysis

The parameter α is a measure of capillary fringe thickness, while n is the pore size distribution of the soil. Both these parameters have significant influence on moisture movement through unsaturated zones. To study the sensitivity of gravity drainage and infiltration to variations in α and n, these are varied over a wide range to cover most of the field soils ranging from sand to clay. Sensitivity analysis is carried out by considering a soil column of 2m thickness.

In the case of gravity drainage (case A), the entire soil profile is initially taken to be fully saturated. Water is allowed to drain due to gravity at the bottom boundary while no flux is allowed at the top boundary. The initial and boundary conditions for gravity drainage are written as

$$
\begin{array}{lll}
t = 0; & \theta = \theta_s, & 0 \le z \le 2\,\text{m}, \\
t > 0; & q_0 = -K, & z = 0, \\
 & q_L = 0, & z = 2\,\text{m},
\end{array}
$$

where q_0 and q_L are Darcy fluxes at the bottom and top boundaries respectively.

For simulating infiltration (case B), the entire soil profile is initially considered to be in very dry condition with a pressure head equal to Ψ_0. A zero pressure head ($\Psi = 0$) is applied at the top and boundary conditions for infiltration are as follows.

$$
\begin{array}{lll}
t = 0; & \Psi = \Psi_0 & 0 \le z \le 2\,\text{m}, \\
t > 0; & \Psi = \Psi_0 & z = 0, \\
 & \Psi = 0 & z = 2\,\text{m}.
\end{array}
$$

5.1 Effect of parameter α

The effect of parameter a is studied by varying α from $0.1\,\text{m}^{-1}$ to $0.3\,\text{m}^{-1}$. The range of a considered here covers most of the field soils. The parameters n, K_s, θ_s and θ_r are kept constant at 2, 0.5 m/day, 0.45 and 0.05 respectively. The values of α considered here are: 0.1, 1, and $3\,\text{m}^{-1}$. Figures 2 and 3 show θ vs ψ and K vs ψ for the α values considered in this study.

Case A – Gravity drainage: Figure 4 shows the moisture content profiles at varies time for different values of α. The parameter α is a measure of capillary fringe thickness of the soil. It can seen from figure 2 that a soil with low a has large capillary fringe thickness. As the value of a increases, thickness of the capillary fringe decreases. Soils with low a values retain considerable amounts of water in the unsaturated zones due to capillary forces. It is observed from figure 4 that at any instant of time, the moisture content is greater for lower values α, than for higher values for the major portion of the column. Moisture content gradients are uniform over the entire soil column for low values of α. As α increases, the gradients tend to become non-uniform at early time with steeper gradients occurring near the soil surface. It is observed that low a values are characterized by lesser gravity drainage and high values with greater drainage.

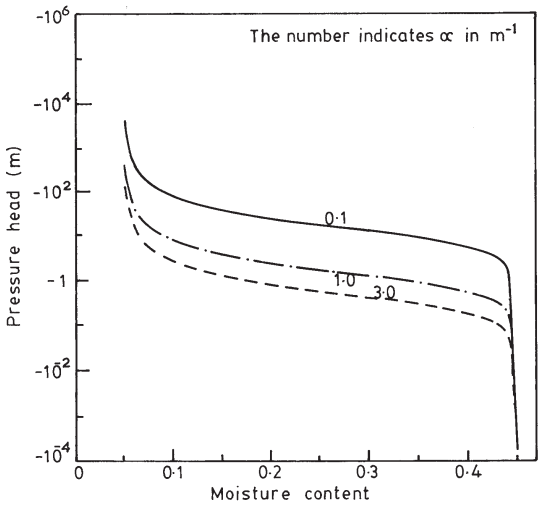

Figure 2. Moisture content–pressure-head relation for different α.

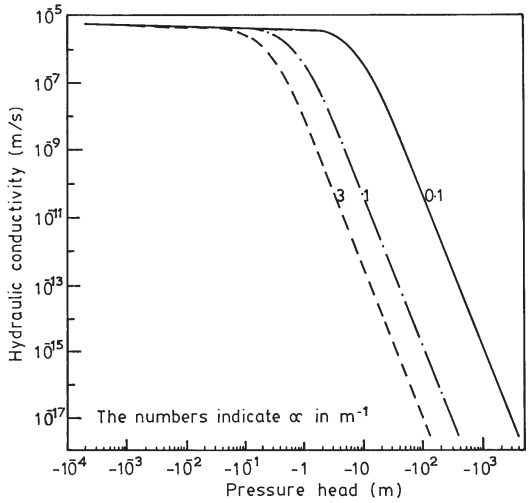

Figure 3. Hydraulic conductivity–pressure head relation for different α.

Case B – Infiltration: Figure 5 shows the pressure head profiles at various times for different values of α. It is seen that as the value of a increases, the wetting front moves at slower rates, since the hydraulic conductivity decreases with increase in α (figure 3) . It is seen from this figure that the wetting front has moved to a greater depth when α is $1\,m^{-1}$ compared to when α is $3\,m^{-1}$ for one day simulation even though the initial pressure heads are chosen such that the initial hydraulic conductivity for both cases is the same. This should be expected as when the soil gets wetted the increase in hydraulic conductivity is higher for low α values. It is of interest to note that the dependence of K on α during the infiltration process plays an important role on the movement of the wetting front.

5.2 Effect of the parameter n

The effect of the parameter n is studied by varying n from 1.5 to 4. The range of n considered here covers most of the field soils. The parameters α, K_s, θ_s and θ_r are kept constant at

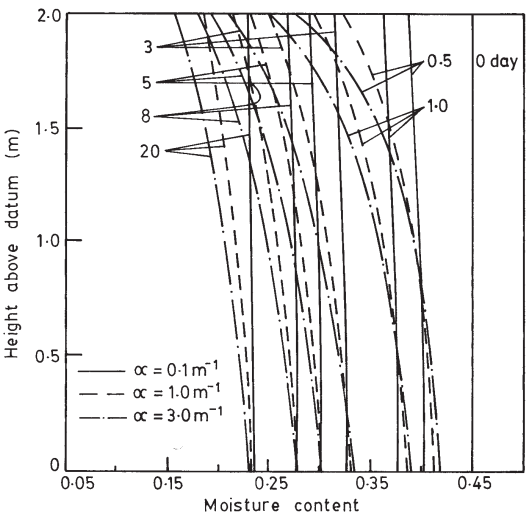

Figure 4. Moisture content profiles – effect of α.

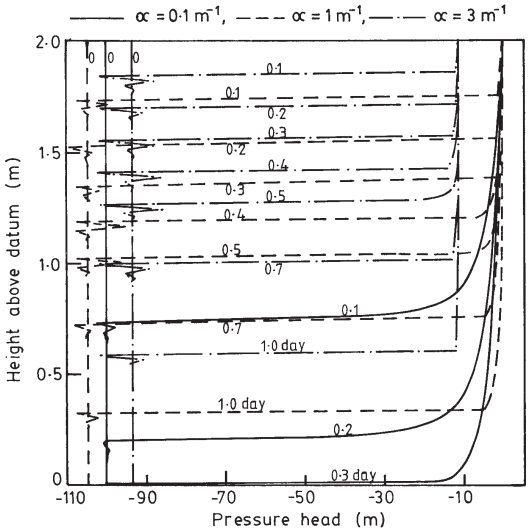

Figure 5. Pressure head distribution–effect of α.

$1\,m^{-1}$, 0.5 m/day, 0.45 and 0.05 respectively. The values of n considered are, $n = 1.5$, 3 and 4. Figures 6 and 7 present θ vs ψ and K vs ψ for the n values considered in this study.

Case A – Gravity drainage: Figure 8 presents the moisture content profiles at various times for different values of n. From figure 6 it is seen that the θ–ψ relationship (SMC) for all n values resembles the pore size distribution of a soil. The parameter n characterizes the width of the pore size distribution. It is observed from figure 6 that as the value of n decreases the width of the pore size distribution increases. Hence with low n values, the relative abundance of small pores increases. These are difficult to drain due to their large viscous effects. This results in slower rate of gravity drainage for low n values as compared to soils with high n values as can be seen from figure 8. It is also observed that the moisture content gradients are non-uniform over the entire soil column for all values of n with steeper gradients occurring near the soil surface. At any instant of time, an increase in n results in a steeper moisture gradient over the soil column.

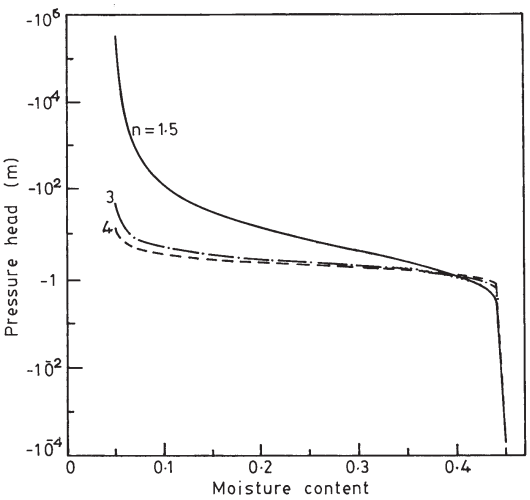

Figure 6. Moisture content–pressure head relation for different n.

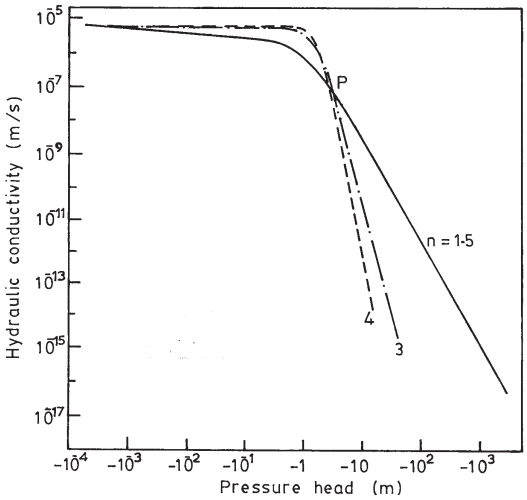

Figure 7. Hydraulic conductivity–pressure head relation for different n.

Case B – Infiltration: Figure 7 shows that as n increases, hydraulic conductivity decreases for all pressure heads less than the value represented by point 'P' in figure 7. Beyond this point the hydraulic conductivity increases with n. Accordingly, the movement of the wetting front during the infiltration process depends on the initial pressure head of the soil column, change in hydraulic conductivity as the soil gets wetted and the pressure head applied at the soil surface. To analyse the effect of n the following cases are considered.

Case B1: Both the initial pressure head for the soil column and the pressure head applied at the soil surface are considered lower than the pressure head at point 'P'.

Case B2: Both the initial pressure head for the soil column and pressure head applied at the soil surface are considered higher than the pressure head at point 'P'.

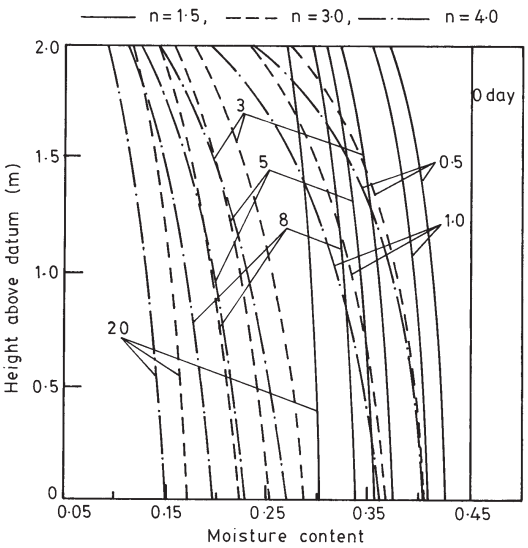

Figure 8. Moisture content profiles – effect of n.

Case B3: The initial pressure head for the soil column is considered lower, while the pressure head applied at the soil surface is considered higher than the value of the pressure head at point 'P'.

Figure 9 shows the 'wetting front' depth for case B1 for different values of n after one day simulation. It is observed in this case that as n increases, the wetting front moves slower. Figure 9 also shows the 'wetting front' depths for different n values for case B2 for 0.1 day simulation. It is observed qualitatively that as n increases the 'wetting front' moves faster in contrast to case B1. However, the changes in wetting front depth for different values of n in figure 9 are small since the changes in hydraulic conductivity for different n are not significant in the pressure head range considered for case B2. Figure 10 shows the pressure head profiles for different values of n for case B3. It can be seen that the wetting front moves at a faster rate as the value of n increases. It is interesting to note that the effect of n on the infiltration process is quite complex from the study of cases B1, B2 and B3 due to the various reasons mentioned above.

6. Application to a field internal drainage test

The model is applied to a field internal drainage test conducted at Adde Viswanathapura near Bangalore in the state of Karnataka in India (Lakshman 1993). The field internal drainage test performed is the same as the gravity drainage problem discussed in sensitivity analysis. The test involves gravity drainage for 20 days from a homogeneous soil wich is initially at near saturation. Based on the studies of Lakshman (1993), the soil parameters at the field site used in the present analysis are: $\alpha = 4.16\,\mathrm{m}^{-1}$, $n = 1.42$, $K_s = 0.15\,\mathrm{m/day}$, $\theta_s = 0.41$ and $\theta_r = 0.11$. Figure 11 presents the field measured moisture contentss using neutron probes at different depths in the soil at different time periods. For simulating the field test, the initial moisture content values for the entire soil depth are obtained using linear interpolation of the measured initial moisture contents at different depths. The field test is simulated using the present model and the computed moisture contents at different depths at various times are also presented in figure 11. It can be seen from figure 11 that a reasonably good fit is obtained between the simulated and the measured moisture contents.

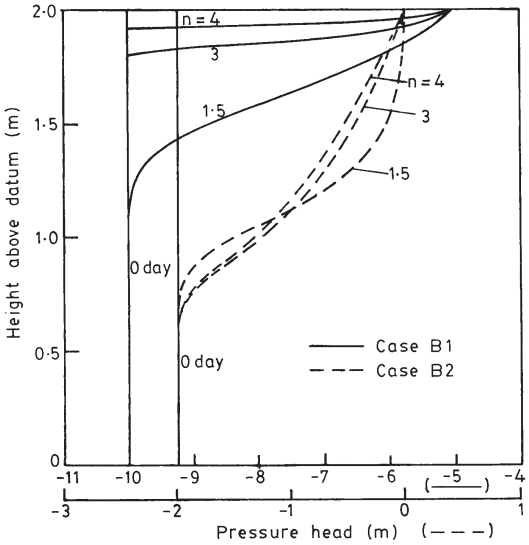

Figure 9. Pressure-head profiles – effect of n – cases B1 and B2.

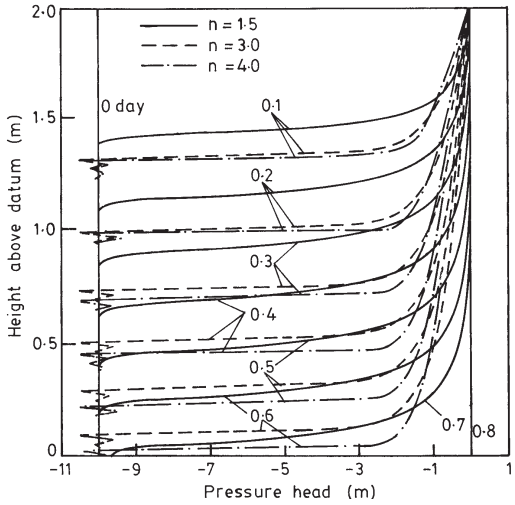

Figure 10. Pressure-head profiles – effect of n – case B3.

7. Conclusions

A numerical flow model is developed for analysing flow moisture through unsaturated zones using the Galerkin fintite element method. The model is validated by comparing the model results with a problem chosen from the literature. Sensitivity analysis is performed to analyse the sensitivity of gravity drainage and infiltration processes to variations in unsaturated soil parameters α and n. It is observed that gravity drainage is slower for low α values as the capillary fringe thickness increases with decreasing values of α, thus storing more water in the unsaturated zones due to capillary forces. During infiltration, as the value of α increases, the wetting front moves at a slower rate since unsaturated hydraulic conductivity decreases with increase in α. As the value of n decreases, the gravity drainage becomes slower, since the relative abundance of small pores, which are difficult to drain, increases. The effect of n on infiltration is complex since the movement of the wetting front depends upon the intial pressure head and the head applied at the top.

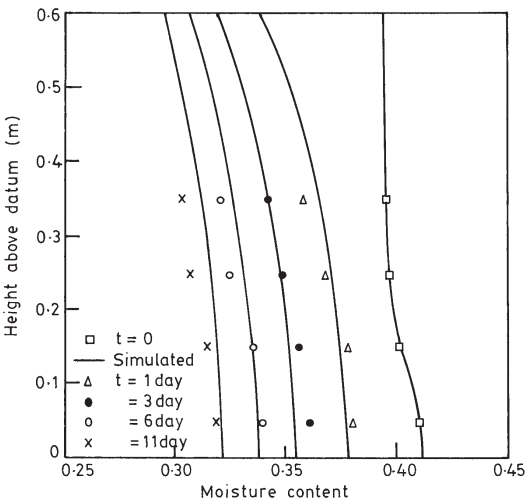

Figure 11. Model fit with field data.

References

Broadbridge P, White I 1988 Constant rate rainfall infiltration: A versatile nonlinear model, 1. Analytical solution. *Water Resour. Res.* 24: 145–154

Celia M A, Bouloutas E T, Zarba R L 1990 A general mass conservative numerical solution for the unsaturated flow equation. *Water Resour. Res.* 26: 1483–1496

Cooley R L 1983 Some new procedures for numerical solution of variably saturated flow problems. *Water Resour. Res.* 19: 1271–1285

Chow V T 1988 *Applied hydrology* (New York: McGraw-Hill)

Chow V T, Maidment D R, Mays L W 1988 *Applied hydrology* Int. Edn (New York: McGraw Hill)

Gottardi G, Venutelli M 1992 Moving finite element model for one dimensional infiltration in unsaturated soil. *Water Resour. Res.* 28: 3259–3267

Hills R G, Porro I, Hudson D B, Wierenga J P 1989 Modeling one dimensional infiltration into very dry soils. 1. Model development and evaluation. *Water Resour. Res.* 25: 1259–1269

Huyakorn P S, Springer E P, Guvansen V, Wordsworth T D 1986 A three dimensional finite element model for simulating water flow in variably saturated porous media. *Water Resour. Res.* 22:1790–1808

Lakshman N 1993 *Field soil moisture regimes and hydrology of irrigated plots.* Ph D thesis, Indian Institute of Science, Bangalore

Narasimhan T N, Witherspoon P A 1977 Numerical model for saturated–unsaturated flow in deformable porous media. 1. Theory. *Water. Resour. Res.* 13: 657–664

Neuman S P 1973 Saturated-unsaturated seepage by finite elements. *J. Hydraul., Am. Soc. Civil Eng.* 99(HY12): 2233–2250

Paniconi C, Aldama A A, Wood E F 1991 Numerical evaluation of iterative and noniterative methods for the solution of nonlinear Richards equation. *Water Resour. Res.* 27: 1147–1163

Parlange J 1972 Theory of water movement in soils, 6, Effect of water depth over soil. *Soil Sci.* 113: 308–312

Philip J R 1969 Theory of infiltration. *Adv. Hydrol. Sci.* 5: 215–296

Richards L A 1931 Capillary conduction of liquids through porous medium. *Physics* 1: 318–313

Remson I, Honberger G M, Molz F J 1971 *Numerical methods in subsurface hydrology* (New York: Wiley-Interscience)

Van Genuchten M T 1980 A closed form equation for predicting the hydraulic conductivity of unsaturated soils. *Soil Sci. Am. J.* 44: 892–898

Warrick A W, Islas A, Lomen D O 1991 An analytical solution to Richards equation for time varying infiltration. *Water Resour. Res.* 27: 763–766